Journal of Multidisciplinary Engineering Science and Technology (JMEST)
ISSN: 3159-0040
Vol. 1 Issue 5, December - 2014

Intelligent Adaptive Motion Control for Ground Wheeled Vehicles

Maurizio Melluso
CIRIAS (Automation Systems Interdepartment Center Research)
University of Palermo, Italy
Viale delle Scienze, 90128, Palermo
Email- maurizio.melluso@alice.it
maurizio.melluso@unipa.it

***Abstract* — In this paper a new intelligent adaptive control is applied to solve a problem of motion control of ground vehicles with two independent wheels actuated by a differential drive. The major objective of this work is to obtain a motion control system by using a new fuzzy inference mechanism where the Lyapunov's stability can be assured. In particular the parameters of the kinematical control law are obtained using an intelligent Fuzzy mechanism, where the properties of the Fuzzy maps have been established to have the stability above. Due to the nonlinear map of the intelligent fuzzy inference mechanism (i.e. fuzzy rules and value of the rule), the parameters above are not constant, but, time after time, based on empirical fuzzy rules, they are updated in function of the values of the tracking errors. Since the fuzzy maps are adjusted based on the control performances, the parameters updating assures a robustness and fast convergence of the tracking errors. Also, since the vehicle dynamics and kinematics can be completely unknown, a dynamical and kinematical adaptive control is added. The proposed fuzzy controller has been implemented for a real nonholonomic electrical vehicle. Therefore system robustness and stability performance are verified through simulations and experimental studies.**

Keywords: Adaptive control, Electric wheeled vehicles, Fuzzy control system, Lyapunov's stability, Motion Control, Nonholonomic systems

I. INTRODUCTION

In recent years much attention has been focused upon the position and orientation control of nonholonomic mechanical systems. Nonholonomic mechanics describes the motion of systems constrained by nonintegrable constraints, i.e. constraints on the system velocities that do not arise from constraints on the configurations alone. A mobile autonomous wheeled vehicle with two wheels actuated by a differential drive mechanism, i.e. two independent electric DC motors with common axis, is usually studied as a typical nonholonomic system. Kinematical nonholonomic constraints arise in wheeled vehicles under the no-slip constraints. Due to nonholonomic motion, the vehicle above is also underactuated [21]. In fact there are three generalized coordinates i.e. lateral position, longitudinal position and vehicle orientation to be controlled, while there are two control inputs only, i.e. steering and longitudinal inputs. Several approaches have been proposed for the synthesis of kinematical controllers for vehicles with nonholonomic constraints on the motion [1], [4], [6]. The kinematical controller is essential to guarantee the vehicle motion along the direction of the orientation. The main idea behind these algorithms is to define velocity control inputs which stabilize the closed loop system. However in many works [5], [6], [7] the parameters of the kinematical control laws are constant and they must be chosen suitably to guarantee the asymptotical stability of the tracking errors. About the dynamical control, backstepping methodologies were treated [6], [10], [20]. Backstepping method is very important since we aim to convert a speed control (high level control) into a torque control (low level control) for the wheels. The classical backstepping control for nonholonomic vehicles implies the knowledge of the kinematical and dynamical parameters. Wavelet Network based controller and techniques of "adaptive backstepping" control have been proposed to solve the problem of unknown parameters and/or unstructured unmodeled dynamics [5], [7], [20]. Relatively few results have been presented about the robustness of the motion control of nonholonomic vehicles [13], i.e. the problem of vehicle control where there are perturbations of the nonholonomic constraints. About the Fuzzy systems, the modern literature is focusing on developing a theory based on Lyapunov's stability. Some researchers [3], [18] provide an interesting theory of stability for Fuzzy Mamdani control systems. About the Fuzzy control applied to nonholonomic vehicles, there are several approaches [2], [11], [12], [17]. However the Lyapunov's stability is not assured. Also the works above are based only on the steering kinematics and assume that there exists *perfect velocity tracking,* i.e. the control signals affect the vehicle velocities instantaneously and this is not true. Some works developed adaptive Fuzzy controller with Lyapunov's stability analysis for manipulators control [14], [15]. About applications to nonholonomic vehicles of Fuzzy control with Lyapunov's stability, relatively few results have been obtained [9], [16].

In this paper, in order to continue this research line, a Fuzzy controller is used to design a stable adaptive kinematical and dynamical control system for a problem of motion control of wheeled autonomous nonholonomic vehicles actuated by a differential drive. This work is an extension of the control strategy proposed in [16].

The contributions of this work include:

1) the use of a new Fuzzy inference mechanism to determine the values of the parameters of the kinematical control laws generating the angular velocities for right and left wheels. So the parameters above are not constant, but they depend on the tracking errors through an intelligent fuzzy system inference, i.e. a set of empirical rules and values of the rules. This assures a good robustness and very good convergence of the motion errors;

2) exhibiting the formal asymptotical stability proof of the motion errors by employing Lyapunov's like Barbalat's theorem based on the input-output properties of the fuzzy inference system.

3) taking the full nonholonomic vehicle dynamics, disturbance and unmodeled dynamics into consideration in the vehicle model and fuzzy control;

4) the extension with an adaptive kinematical and dynamical control and asymptotical stability proof of the adaptive control scheme. In this way the kinematical and dynamical parameters of the vehicle model can be unknown;

5) simulation to verify the robustness and the asymptotical stability of the motion errors;

6) implementation of the controller and application to a real nonholonomic vehicle to verify the validity of the method.

This paper is organized as it follows. Section II describes the kinematic and dynamic model of a vehicle with nonholonomic constraints. Section III.A presents the fundamental innovation of this paper i.e. the new adaptive fuzzy speed system for motion control of nonholonomic autonomous vehicles. The inputs of the fuzzy system are the tracking errors of the motion control system, while the crisp outputs are the parameters of the kinematic control law. Due to the road conditions and contact between the wheels and the ground, the impact of the vehicle with the environment can cause slipping of the wheels with consequential perturbations violating the nonholonomic constraints. By using our fuzzy solution, the constant parameters of the classical kinematic control law [6] are obviated. In fact, in our approach, the parameters above are nonlinear functions of the tracking errors and this assures a certain robustness with respect to the perturbations above and faster convergence than the adaptive controller shown in [7]. In particular, by inserting the input-output functions of the fuzzy map without approximation into kinematic control law suitably, the input-output properties of the fuzzy system are determined to guarantee the asymptotical stability of the tracking errors which has been proved in Section III.B. Section III.C adds an adaptive kinematical control with stability proof. So the kinematical parameters of the vehicle model may be unknown. In Section IV a dynamical extension and an adaptive control are presented with stability proof. Several parameters of the dynamic model (i.e. mass, friction, other disturbances) are unknown; therefore an adaptation is explained by employing the adaptive backstepping method suitably. In Section V some simulation tests in Matlab environment illustrate the robustness and the asymptotical stability of the tracking errors for the proposed fuzzy control system and we compare our results with the adaptive control without fuzzy proposed in [7]. Section VI shows experimental results obtained by an implementation of the proposed control system for a real nonholonomic vehicle. Section VII presents our conclusion.

II. MATHEMATICAL MODEL OF GROUND VEHICLES

In this section forms of the kinematic and dynamic model of a nonholonomic vehicle are presented to develop the control system of the next sections.

Let us consider a mobile nonholonomic vehicle (see Fig. 1) with generalized coordinates $\mathbf{q} \in \Re^n$, subject to m constraints. The well known dynamic model [6] is:

$$\mathbf{M}(\mathbf{q})\ddot{\mathbf{q}} + \mathbf{C}(\mathbf{q},\dot{\mathbf{q}})\dot{\mathbf{q}} + \boldsymbol{\tau}_d = \mathbf{E}(\mathbf{q})\boldsymbol{\tau} - \mathbf{A}^T(\mathbf{q})\boldsymbol{\lambda} \quad (1)$$

where:

$\mathbf{M}(\mathbf{q}) \in \Re^{n\times n}$ is a symmetric, positive definite matrix; $\mathbf{C}(\mathbf{q},\dot{\mathbf{q}}) \in \Re^{n\times n}$ is the centripetal Coriolis matrix;

$\boldsymbol{\tau}_d \in \Re^n$ is a bounded unknown disturbance including unstructured and unmodeled dynamics;

$\boldsymbol{\tau} \in \Re^r$ is the input vector including torques applied to right and left wheel;

$\mathbf{A}(\mathbf{q}) \in \Re^{m\times n}$ is the matrix of nonholonomic constraints;

$\mathbf{E}(\mathbf{q}) \in \Re^{n\times r}$ is the input transformation matrix;

$\boldsymbol{\lambda} \in \Re^m$ is the Lagrange multiplier vector of constraint forces.

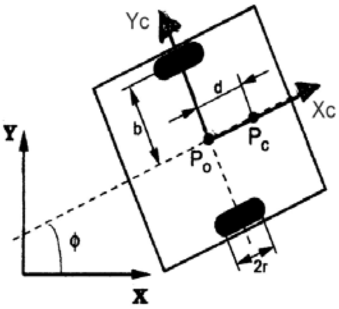

Fig. 1. Nonholonomic vehicle and coordinate systems

Supposing that the *m* constraints are time invariant, it yields:

$$\mathbf{A}(\mathbf{q})\dot{\mathbf{q}} = \mathbf{0} \tag{2}$$

Let **S(q)** be the Jacobian matrix with full rank $n \times (n-m)$ and made up by a set of smooth and linearly independent vectors spanning the null space of $\mathbf{A}(\mathbf{q})$ i.e.:

$$\mathbf{A}(\mathbf{q})\mathbf{S}(\mathbf{q}) = \mathbf{0} \tag{3}$$

It is possible to find a (*n-m*) velocity vector **v** as it follows:

$$\mathbf{v}^{\mathbf{T}} = [u \ \ \omega] \tag{4}$$

where *u* and ω are the linear and angular body-fixed (*Xc,Yc*) velocities of the nonholonomic vehicle (see Fig. 1). About the kinematical parameters, let *r* and *b* be the ray of the wheels and the distance between the driving wheels and the axis of symmetry. The P_0 coordinates, *i.e.* the intersection of the axis of symmetry with the driving wheel axis (see Fig. 1), are indicated by (x_0, y_0), while the vehicle orientation is indicated by

□. In this way we focus only on three

variables x, y, ϕ, excluding the angular velocities of the right wheel ($\dot{\theta}_r$) and of the left wheel ($\dot{\theta}_l$).The relationship between the vector $[u \ \ \omega]$ and the vector $[\dot{\theta}_r \ \ \dot{\theta}_l]$ is the following:

$$\begin{bmatrix} \dot{\theta}_r \\ \dot{\theta}_l \end{bmatrix} = \begin{bmatrix} \frac{1}{r} & \frac{b}{r} \\ \frac{1}{r} & \frac{-b}{r} \end{bmatrix} \begin{bmatrix} u \\ \omega \end{bmatrix} \tag{5}$$

Equations (5) can be rewritten as it follows:

$$\boldsymbol{\eta} = \begin{bmatrix} \frac{1}{r} & \frac{b}{r} \\ \frac{1}{r} & \frac{-b}{r} \end{bmatrix} \mathbf{v} \tag{6}$$

where:

$$\boldsymbol{\eta}^{\mathbf{T}} = [\ \dot{\theta}_r \ \ \dot{\theta}_l \ ] \tag{7}$$

Therefore, the model of a nonholonomic vehicle can be described employing five generalized coordinates:

$$\mathbf{q}^{\mathbf{T}} = [\ x_0 \ \ y_0 \ \ \phi \ \ \theta_r \ \ \theta_l \ ] \tag{8}$$

In the condition of pure rolling and non-slipping, the vehicle can move in perpendicular direction to the driving wheels axis. So we have three constraint equations of the vehicle motion:

$$\begin{aligned} &\dot{x}_0 \sin\phi - \dot{y}_0 \cos\phi = 0 \\ &\dot{x}_0 \cos\phi + \dot{y}_0 \sin\phi + b\dot{\phi} = r\dot{\theta}_r \\ &\dot{x}_0 \cos\phi + \dot{y}_0 \sin\phi - b\dot{\phi} = r\dot{\theta}_l \end{aligned} \tag{9}$$

The constraints above can be written in *pfaffian* form (2). From equation (3), the Jacobian matrix $\mathbf{S}(\mathbf{q})$ is:

$$\mathbf{S}^{\mathbf{T}}(\mathbf{q}) = \begin{bmatrix} cb\cos\phi & cb\sin\phi & c & 1 & 0 \\ cb\cos\phi & cb\sin\phi & -c & 0 & 1 \end{bmatrix} \tag{10}$$

where *c=r/2b.*

One of three constraints (9) is holonomic [19]. In fact, by comparing the second and third of equations (9), it follows:

$$\dot{\phi} = c(\dot{\theta}_r - \dot{\theta}_l) \tag{11}$$

The constraint (11) is integrable. Therefore, by eliminating ϕ or θ_r and θ_l in vector (8), two new vectors of generalized coordinates can be defined:

$$\mathbf{q}_1^{\mathbf{T}} = [\ x_0 \ \ y_0 \ \ \theta_r \ \ \theta_l \ ] \tag{12}$$

or

$$\mathbf{q}_2^{\mathbf{T}} = [\ x_0 \ \ y_0 \ \ \phi \ ] \tag{13}$$

In cases (12) and (13) $\mathbf{A}(\mathbf{q})$ matrix presents nonholonomic constraints only. In particular, in case (12), a new Jacobian matrix is obtained as it follows:

$$\mathbf{S}_1^{\mathbf{T}}(\mathbf{q}_1) = \begin{bmatrix} c^2 b\cos(\theta_r - \theta_l) & c^2 b\sin(\theta_r - \theta_l) & 1 & 0 \\ c^2 b\cos(\theta_r - \theta_l) & c^2 b\sin(\theta_r - \theta_l) & 0 & 1 \end{bmatrix} \tag{14}$$

In this way the kinematic model is:

$$\dot{\mathbf{q}}_1 = \mathbf{S}_1(\mathbf{q}_1)\boldsymbol{\eta} \tag{15}$$

In case (13) the kinematic model is:

$$\begin{bmatrix} \dot{x}_0 \\ \dot{y}_0 \\ \dot{\phi} \end{bmatrix} = \begin{bmatrix} cb\cos\phi & cb\cos\phi \\ cb\sin\phi & cb\sin\phi \\ c & -c \end{bmatrix} \begin{bmatrix} \dot{\theta}_r \\ \dot{\theta}_l \end{bmatrix} \tag{16}$$

From (4) and (13) and, by substituting equation (6) into (16), it yields:

$$\dot{\mathbf{q}}_2 = \mathbf{S}_2(\mathbf{q}_2)\mathbf{v} \tag{17}$$

where:

$$\mathbf{S}_2(\mathbf{q}_2) = \begin{bmatrix} \cos\phi & 0 \\ \sin\phi & 0 \\ 0 & 1 \end{bmatrix}$$

About the dynamical parameters, let P_c be the mass center of the vehicle which is on the X-axis, let *d* be the distance from P_0 to P_c (see Fig. 1). For the later description, m_c is the mass of the vehicle without the driving wheels, m_w is the mass of each driving wheels, I_c, I_w and I_m are the inertia moments of the body around a vertical axis through P_0, of the wheel with a motor around the wheel axis and of the wheel with a motor around the wheel diameter, respectively. Now the dynamical model in body-fixed coordinates (*Xc, Yc*) is obtained by differentiating (15), replacing it into (1) and performing additional operations with $\mathbf{S_1}$. It follows:

$$\mathbf{S}_1^T\mathbf{M}(\mathbf{q}_1)\mathbf{S}_1\dot{\boldsymbol{\eta}} + \mathbf{S}_1^T(\mathbf{M}(\mathbf{q}_1)\dot{\mathbf{S}}_1 + \mathbf{C}(\mathbf{q}_1,\dot{\mathbf{q}}_1)\mathbf{S}_1)\boldsymbol{\eta} = \\ = \mathbf{S}_1^T\mathbf{E}(\mathbf{q}_1)\boldsymbol{\tau} - \mathbf{S}_1^T\boldsymbol{\tau}_\mathbf{d}$$

or

$$\overline{\mathbf{M}}\dot{\boldsymbol{\eta}} + \overline{\mathbf{V}}_\mathbf{m}(\boldsymbol{\eta})\boldsymbol{\eta} = \mathbf{B}\boldsymbol{\tau} - \mathbf{S}_1^\mathbf{T}\boldsymbol{\tau}_d \tag{18}$$

where:

$$\overline{\mathbf{M}} = \begin{bmatrix} b^2c^2m + c^2I + I_w & b^2c^2m - c^2I \\ b^2c^2m - c^2I & b^2c^2m + c^2I + I_w \end{bmatrix} \tag{19}$$

$$\overline{\mathbf{V}}_\mathbf{m}(\boldsymbol{\eta}) = \begin{bmatrix} 0 & 2bc^3dm_c(\dot{\theta}_r - \dot{\theta}_l) \\ -2bc^3dm_c(\dot{\theta}_r - \dot{\theta}_l) & 0 \end{bmatrix}$$

$$\mathbf{B} = \begin{bmatrix} 1 & 0 \\ 0 & 1 \end{bmatrix}; \quad \boldsymbol{\tau} = \begin{bmatrix} \tau_r \\ \tau_l \end{bmatrix}$$

and *m* and *I* are the dynamical parameters as it follows:

$$m = m_c + 2m_w; \quad I = m_c d^2 + I_c + 2m_w b^2 + 2I_m$$

Also $\overline{\mathbf{M}} \in \Re^{(n-m)\times(n-m)}$ is a symmetric and definite positive matrix, while $\overline{\mathbf{V}}_\mathbf{m}(\boldsymbol{\eta})\boldsymbol{\eta} \in \Re^{(n-m)\times 1}$.

III. ADAPTIVE INTELLIGENT CONTROL OF GROUND VEHICLES

In this section the fundamental innovation of this paper is presented, i.e. a new fuzzy adaptive motion control system for electric nonholonomic vehicles with two independent wheels.

A. *Intelligent kinematic control*

Let the references of velocities and positions for a nonholonomic vehicle be:

$$\begin{aligned} \dot{x}_r &= u_r \cos\phi_r \\ \dot{y}_r &= u_r \sin\phi_r \\ \dot{\theta}_r &= \omega_r \end{aligned} \tag{20}$$

where u_r>0 is the reference linear velocity and □s the reference angular velocity. The tracking errors between the reference position $\mathbf{q}_\mathbf{r}^\mathbf{T} = [x_r, y_r, \phi_r\ ]$ and the actual position $\mathbf{q}^\mathbf{T} = [x, y, \phi\ ]$ can be expressed in the vehicle local frame (*Xc, Yc*) as [6]:

$$\mathbf{e} = \begin{bmatrix} e_x \\ e_y \\ e_\phi \end{bmatrix} = \begin{bmatrix} \cos\phi & \sin\phi & 0 \\ -\sin\phi & \cos\phi & 0 \\ 0 & 0 & 1 \end{bmatrix} \begin{bmatrix} x_r - x \\ y_r - y \\ \phi_r - \phi \end{bmatrix} \tag{21}$$

where e_x and e_y are the lateral and longitudinal position errors, while $e_{\square}$ is the vehicle orientation error. Note that, time after time, the vector $\mathbf{q_r}$(t) is the reference motion for the vehicle, while **q**(t) is the real motion of the vehicle above. So, differentiating equation system (21) and applying two auxiliary inputs:

$$u_1 = -u_c + u_r \cos e_\phi\,; \quad u_2 = \omega_r - \omega_C \tag{22}$$

where u_c and ω_c are the kinematic control laws in terms of steering and longitudinal velocities lead to:

$$\begin{bmatrix} \dot{e}_x \\ \dot{e}_y \\ \dot{e}_\phi \end{bmatrix} = \begin{bmatrix} 0 & \omega_c & 0 \\ -\omega_c & 0 & 0 \\ 0 & 0 & 0 \end{bmatrix} \begin{bmatrix} e_x \\ e_y \\ e_\phi \end{bmatrix} + \begin{bmatrix} 0 \\ u_r \sin e_\phi \\ 0 \end{bmatrix} + \begin{bmatrix} 1 & 0 \\ 0 & 0 \\ 0 & 1 \end{bmatrix} \begin{bmatrix} u_1 \\ u_2 \end{bmatrix} \tag{23}$$

Now a new fuzzy kinematic control law is proposed:

$$\begin{aligned} u_c &= u_r \cos e_\phi + k_x(t) e_x \\ \omega_c &= \omega_r + u_r (k_y(t) e_y + k_\phi(t) \sin e_\phi) \end{aligned} \tag{24}$$

This control law depends on the error vector (21) and on the following parameters:

$$\mathbf{k}^\mathbf{T} = [\ k_x(t)\ \ k_y(t)\ \ k_\phi(t)\ ] \tag{25}$$

Parameters (25) are provided by a fuzzy controller. The fuzzy controller is used because, in this way, the parameters of the kinematic control law are not constant as in the controllers proposed in [6] and [7], but they are nonlinear functions of the tracking errors (21) through an intelligent fuzzy inference system, i.e. empirical Fuzzy rules and values of the rules. In other words, since the model of the nonholonomic vehicle is highly nonlinear, it is convenient to have nonlinear functions of the tracking errors in the control laws. Since the fuzzy maps are adjusted based on the control performance, the updating of the parameters (25) assures a good robustness and fast convergence. Now the Fuzzy inference system is described. The input and output membership functions are shown in Figs. 2, 3 respectively. The fuzzy rules are shown in Fig. 4. The input and output memberships are *generalized bell* functions and three linguistic labels are defined:

S=Small; M=Medium; H=High; Opp=Opposite.

The inputs of the fuzzification process (see Fig. 2) are the absolute values of the tracking errors (cf. eq. 21), while the outputs of the input memberships are the degree of membership in the qualifying linguistic sets (always the interval between 0 and 1). The input set is a fuzzy singleton. The implemented methods for the logical 'and' and for the implication are the "minimum" and the "fuzzy minimum" respectively. The "fuzzy minimum" method truncates the output fuzzy set opportunely. Since decisions are based on testing of all the rules (see Fig. 4), the aggregation is necessary; therefore the consequents of each rule have been recombined using a *maximum (max)* method. The used defuzzification method is the "centroid". So the outputs of the fuzzy system are crisp values *i.e*. the parameters (25) (see Fig. 3).

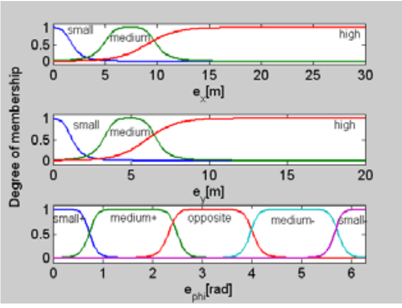

Fig. 2. Input membership functions

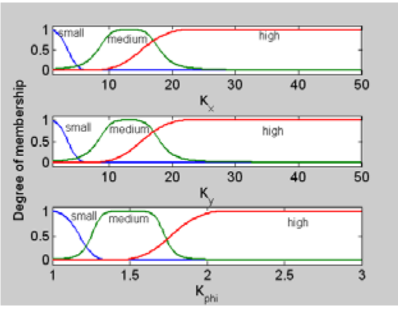

Fig. 3. Output membership functions

TABLE I
CONTROLLER RULES

N° RULES	E_X	E_Y	E_Φ	K_X	K_Y	K_ϕ
1	S	S	S+	S	S	S
2	S	M	S+	S	M	S
3	S	H	S+	M	H	S
4	M	S	S+	M	S	S
5	M	M	S+	M	M	S
6	M	H	S+	M	H	S
7	H	S	S+	H	M	S
8	H	M	S+	H	M	S
9	H	H	S+	H	H	S
10	S	S	M+	M	M	M
11	S	M	M+	M	M	M
12	S	H	M+	M	H	M
13	M	S	M+	M	M	M
14	M	M	M+	M	M	M
15	M	H	M+	M	H	M
16	H	S	M+	H	M	M
17	H	M	M+	H	M	M
18	H	H	M+	H	H	M
19	S	S	OPP	M	M	H
20	S	M	OPP	M	M	H
21	S	H	OPP	M	H	H
22	M	S	OPP	M	M	H
23	M	M	OPP	M	M	H
24	M	H	OPP	M	H	H
25	H	S	OPP	H	M	H
26	H	M	OPP	H	M	H
27	H	H	OPP	H	H	H
28	S	S	M-	M	M	M
29	S	M	M-	M	M	M
30	S	H	M-	M	H	M
31	M	S	M-	M	M	M
32	M	M	M-	M	M	M
33	M	H	M-	M	H	M
34	H	S	M-	H	M	M
35	H	M	M-	H	M	M
36	H	H	M-	H	H	M
37	S	S	S-	S	S	S
38	S	M	S-	S	M	S
39	S	H	S-	M	H	S
40	M	S	S-	M	S	S
41	M	M	S-	M	M	S
42	M	H	S-	M	H	S
43	H	S	S-	H	M	S
44	H	M	S-	H	M	S
45	H	H	S-	H	H	S

Fig. 4. Table of the rules

Remark 1. The numerical outputs of the fuzzy inference system depend on the tracking errors (21), therefore they are time varying functions (cf. eq. 25).

Remark 2. Since the parameters (25) depend on the tracking errors, the control system of this paper can be more robust and with faster convergence than the conventional controllers [6], [7], where the parameters of the kinematic control law are constant numbers.

Remark 3. About the memberships this remark is essential. The generalized bell functions have been chosen for the smoothness which assures continuous functions to guarantee the Lyapunov's stability of the control system.

Remark 4. The parameters k_x k_y and k_{ϕ} positive numbers (see Fig. 3) always to assure the stability.

Remark 5. Note that the numerical inputs of the fuzzy system (cfr. Fig. 2) are the absolute values of the tracking errors (the range of the errors is constituted by positive values only). In any case the sign (positive or negative) of the errors above is considered by the fuzzy control laws (24).

Now Figs. 5 and 6 show the Fuzzy control surfaces. In particular the plots above show the output k_y of the Fuzzy inference mechanism versus two of the inputs. In other words figs 5 and 6 show the fuzzy map, where the parameter k_y depends on the tracking errors (21) trough the Fuzzy inference system which has been described. So the maps of Figs 5 and 6 depend on the fuzzy inference system, i.e. empirical rules and value of the rules. To assure the Lyapunov's stability of the motion control system, one must investigate on the input-output properties of the fuzzy system. So, from Figs. 2, 3, 5, 6, the properties of the parameters (25) are the following.

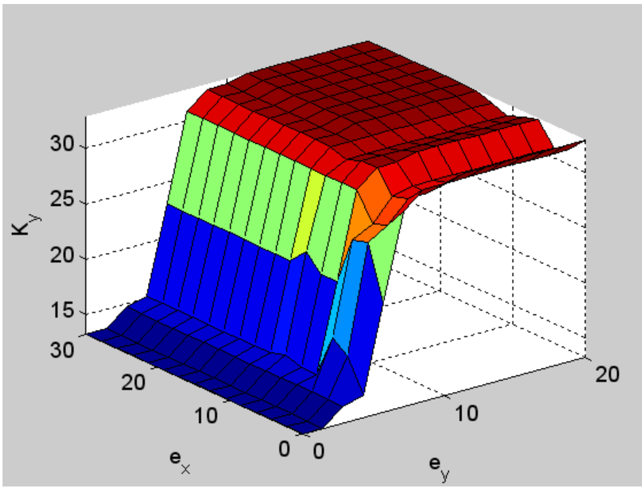

Fig. 5. k_y versus e_x and e_y

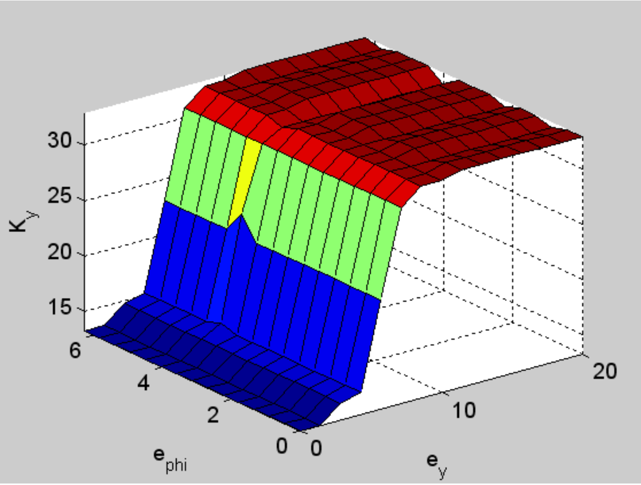

Fig.6. k_y versus e_ϕ and e_y

Property 1.a. The parameters of the kinematical control law (25) are continuous time functions;

Property 2.a. The vector **k(e**(t)**)** (cf. eq. 25) is equal to zero if only if **e** is equal to zero *i.e.*:

$$\mathbf{k}^{\mathbf{T}}(\mathbf{e}(t)) = \begin{bmatrix} k_x(t) & k_y(t) & k_\phi(t) \end{bmatrix} = \mathbf{0} \Leftrightarrow \mathbf{e} = \mathbf{0};$$

Property 3.a. All the outputs of the Fuzzy inference system are positive numbers and are bounded *i.e.*:

$$0 \le k_x(t) \le k_{x\max} \quad ; \quad 0 \le k_y(t) \le k_{y\max}$$
$$0 \le k_\phi(t) \le k_{\phi\max};$$

Property 4.a. Considering $j \in N$ and *M>0* and taking into account property 3.a lead to:

$$\sum_{j=0}^{M-1}\left[\int_j^{j+1} k_y(t)dt\right] > 0$$

Now replacing fuzzy control law (24) into model (23) leads to:

$$\dot{\mathbf{e}}^{\mathbf{T}} = \begin{bmatrix} \dot{e}_x & \dot{e}_y & \dot{e}_\phi \end{bmatrix} =$$
$$\begin{bmatrix} (\omega_r + u_r(k_y(t))e_y + k_\phi(t)\sin e_\phi)e_y - k_x(t)e_x \\ -(\omega_r + u_r(k_y(t))e_y + k_\phi(t)\sin e_\phi)e_x + u_r \sin e_\phi \\ -u_r(k_y(t)e_y + k_\phi(t)\sin e_\phi) \end{bmatrix} \quad (26)$$

B. Lyapunov's stability proof based on the input output properties of the fuzzy system

From the Fuzzy inference system, equations and properties so far, it follows the first main result of this work.

Theorem 1: Let the kinematical model and the fuzzy kinematical control laws be (17) and (24) respectively. Let the linear reference velocity u_r be positive. The properties 1.a - 4.a are verified for hypothesis. Then the equilibrium state of the non autonomous closed loop system (26) is the origin of the state space and it is asymptotically stable.

Proof. Since the vector $\mathbf{k}(\mathbf{e})$ (cf. eq. 25) is equal to zero if only if $\mathbf{e}$ is equal to zero, the equilibrium state of the closed loop system (26) is the origin of the state space. The system (26) is non autonomous. The following Lyapunov's function is chosen:

$$V_0 = \frac{1}{2}(e_x^2 + e_y^2) + (1-\cos e_\phi)\sum_{j=0}^{M-1}\left[\int_j^{j+1} k_y(t)dt\right] \quad (27)$$

where :

$$j \in N, M > 0 \quad (28)$$

For hypothesis it is:

$$\sum_{j=0}^{M-1}\left[\int_j^{j+1} k_y(t)dt\right] > 0 \quad (29)$$

Therefore the Lyapunov's function (27) is positive definite.

The time derivative of (27) is:

$$\dot{V}_0 = e_x\dot{e}_x + e_y\dot{e}_y + \dot{e}_\phi \sin e_\phi \sum_{j=0}^{M-1}\left[\int_j^{j+1} k_y(t)dt\right] +$$
$$+ (1-\cos e_\phi)\frac{d}{dt}\left(\sum_{j=0}^{M-1}\left[\int_j^{j+1} k_y(t)dt\right]\right) \quad (30)$$

where:

$$\frac{d}{dt}\left(\sum_{j=0}^{M-1}\left[\int_j^{j+1} k_y(t)dt\right]\right) = \sum_{j=0}^{M-1} k_y(j) \quad (31)$$

By substituting (26) into (30), it yields:

$$\dot{V}_0 = -k_x(t)e_x^2 - u_r k_\phi(t)\sin^2(e_\phi)\sum_{j=0}^{M-1}\left[\int_j^{j+1} k_y(t)dt\right] +$$
$$+ (1-\cos e_\phi)\sum_{j=0}^{M-1} k_y(j) \quad (32)$$

Due to properties (3.a) and (4.a) of the Fuzzy map, the first and second terms of (32) are negative. Also it results:

$$u_r k_\phi(t)(1-\cos^2 e_\phi)\times$$
$$\times \sum_{j=0}^{M-1}\int_j^{j+1} k_y(t)dt > (1-\cos e_\phi)\sum_{j=0}^{M-1} k_y(j) \quad (33)$$

Since the function (33) does not depend on e_y error, it is negative semidefinite. Therefore vector (21) is bounded and the equilibrium state of the closed loop system (26) is stable. It is also possible to calculate the second time derivative of Lyapunov's function (27). Since the second time derivative of (27) depends on bounded variables, it is a bounded function. Therefore the function (32) is uniformly continuous. From Barbalat's Lemma [8], it yields:

$$\lim_{t\to\infty}\dot{V}_0(t)=0 \tag{34}$$

From equations (32) and (34), e_x and e_ϕ converge to zero. From the second equation of (26) that is:

$$\dot{e}_y=-(\omega_r+u_r(k_y(t)e_y+k_\phi(t)\sin e_\phi)e_x+u_r\sin e_\phi \tag{35}$$

The function $\dot{e}_y$ converges to zero. Therefore the steady state error along *y* direction is constant. Examining the third equation of (26) leads to:

$$\dot{e}_\phi(\infty)=-u_r k_y(\infty)\bar{e}_y \tag{36}$$

where $\bar{e}_y$ is the steady state value of e_y. Since e_ϕ converges to zero, e_y converges to zero. Now k_y is equal to zero if $\bar{e}_y$ is equal to zero. Therefore the equilibrium point of the closed loop system (26) is asymptotically stable Q.E.D.

Remark 6. Note that the proof of the theorem 1 requires the system kinematical parameters of the vehicle be accurately known.

C. Intelligent Adaptive Kinematic Control

In this subsection the second main result of this work is explained. An adaptive controller is added to previous fuzzy control and the stability is proved. This step is necessary because the kinematical parameters as the ray of the wheels and particularly the distance between the driving wheels and the axis of symmetry can be difficult to be determined accurately. In fact without adaptive control one must measure the parameters above manually and this can cause a measurement error perturbing the performances of the control system. Fig. 7. shows the block diagram of the fuzzy adaptive control system.

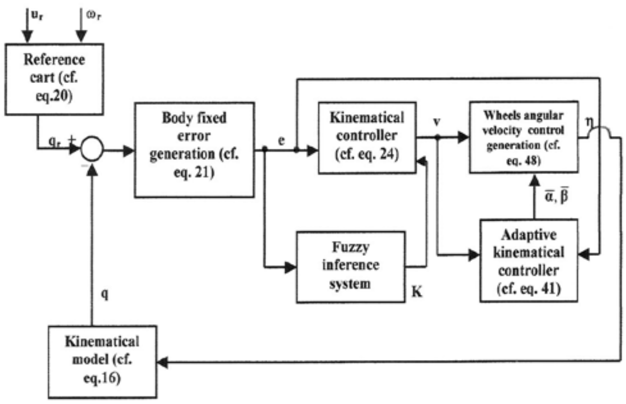

Fig. 7. Block diagram of the fuzzy adaptive kinematic control system

Preliminarily, from (6), (16), (23) and after simple calculations, the closed loop kinematical control system can be written in the following way:

$$\frac{d}{dt}\begin{bmatrix}e_x\\e_y\\e_\phi\end{bmatrix}=\dot{\theta}_r\begin{bmatrix}-\frac{r}{2}+\frac{r}{2b}e_y\\-\frac{r}{2b}e_x\\-\frac{r}{2b}\end{bmatrix}+\dot{\theta}_l\begin{bmatrix}-\frac{r}{2}-\frac{r}{2b}\\\frac{r}{2b}e_x\\\frac{r}{2b}\end{bmatrix}+\begin{bmatrix}u_r\cos(e_\phi)\\u_r\sin(e_\phi)\\\omega_r\end{bmatrix} \tag{37}$$

We set:

$$\alpha=1/r;\ \ \beta=b/r \tag{38}$$

Differential equations (37) can be exploited by considering the estimation errors of the kinematical parameters (38):

$$\hat{\alpha}=\bar{\alpha}-\alpha;\ \ \hat{\beta}=\bar{\beta}-\beta \tag{39}$$

where $\bar{\alpha}$ and $\bar{\beta}$ are the estimated values. It results:

$$\frac{d}{dt}\begin{bmatrix}e_x\\e_y\\e_\phi\end{bmatrix}=\left(1+\frac{\hat{\alpha}}{\alpha}\right)u_c\begin{bmatrix}-1\\0\\0\end{bmatrix}+\left(1+\frac{\hat{\beta}}{\beta}\right)\omega_c\begin{bmatrix}e_y\\-e_x\\-1\end{bmatrix}+ \tag{40}$$
$$+\left[u_r\cos(e_\phi)\ \ u_r\sin(e_\phi)\ \ \omega_r\right]^{\mathrm{T}}$$

Now it is possible to formulate the following theorem.

Theorem 2: Let the kinematical model and the fuzzy control law be (17) and (24) respectively. If the reference linear and angular velocities are bounded functions and the reference angular velocity converges to zero, by choosing of the following adaptive kinematic control law:

$$\dot{\bar{\alpha}}=\gamma e_x u_c\quad \dot{\bar{\beta}}=\delta\frac{\omega_c\sin(e_\phi)}{k_y(t)}\qquad \gamma,\delta>0 \tag{41}$$

the components of the vector $[\ e_x,e_y,e_\phi\ ]^T$ of the closed loop system (40) converge to zero.

Proof. An extended state vector can be defined:

$$\mathbf{\bar{e}}^{\mathrm{T}}=[\ e_x\ \ e_y\ \ e_\phi\ \ \hat{\alpha}\ \ \hat{\beta}\ ] \tag{42}$$

The Lyapunov's function can be chosen as it follows:

$$V_1=V_0+\frac{1}{2\gamma\alpha}\hat{\alpha}^2+\frac{1}{2\delta\beta}\hat{\beta}^2 \tag{43}$$
$$\gamma,\delta>0$$

where V_0 is given by (27). Since V_0 is positive definite, it is obvious that V_1 is positive definite. Substituting the fuzzy control law (24) into (41) and differentiating (43) lead to:

$$\dot{V}_1 = \dot{V}_0 + \frac{\hat{\alpha}}{\gamma\alpha}(\dot{\bar{\alpha}} - \gamma e_x u_c) + \frac{\hat{\beta}}{\delta\beta}(\dot{\bar{\beta}} - \delta \frac{\omega_c \sin(e_\phi)}{k_y(t)}) \quad (44)$$

where u_c and ω_c are given by (24) and $\dot{V}_0$ is given by (32). Function (44) is negative semidefinite if and only if equations (41) are verified. In this case it results:

$$\dot{V}_1 = \dot{V}_0 \quad (45)$$

Since the function (45) does not depend on e_y component (cf. eq. 32), it is negative semidefinite. Therefore the closed loop system (40) is stable and the components of the state vector (42) are bounded. It is also possible to calculate the second time derivative of Lyapunov's function (43). Since it depends on bounded variables, from Barbalat's Lemma it results:

$$\lim_{t\to\infty} \dot{V}_1(t) = 0 \quad (46)$$

Therefore e_x and e_ϕ converge to zero. Now, by substituting (24) into (40), it results:

$$\dot{e}_\phi = -\left(1 + \frac{\hat{\beta}}{\beta}\right)(\omega_r + u_r k_y(t) e_y + k_\phi(t)\sin(e_\phi)) + \omega_r \quad (47)$$

Since the reference linear velocity u_r, the reference angular velocity ω_r and the components of state vector (42) are bounded, $\ddot{e}_\phi$ is bounded. Therefore $\dot{e}_\phi$ is uniformly continuous. Since e_ϕ converges to zero, from Barbalat's Lemma, $\dot{e}_\phi$ converges to zero; therefore from (47) e_y converges to zero only if ω_r converges to zero Q.E.D.

Remark 7. From the previous results, the adaptive fuzzy kinematic control law can be written in terms of angular velocities of left ($\dot{\theta}_{lc}$) and right ($\dot{\theta}_{rc}$) wheels as it follows:

$$\boldsymbol{\eta}_\mathbf{c} = \begin{bmatrix} \dot{\theta}_{rc} \\ \dot{\theta}_{lc} \end{bmatrix} = \begin{bmatrix} \bar{\alpha} & \bar{\beta} \\ \bar{\alpha} & -\bar{\beta} \end{bmatrix} \begin{bmatrix} u_c \\ \omega_c \end{bmatrix} \quad (48)$$

where $\bar{\alpha}$ and $\bar{\beta}$ are the solutions of the differential equations (41), while u_c and ω_c are the fuzzy control laws given by (24). For theorems 1 and 2, by employing the adaptive fuzzy kinematic control law (48), the closed loop motion control system of the nonholonomic vehicle is asymptotically stable.

Remark 8. Note that, if the kinematic adaptive control law (48) is applied to vehicle directly, then the perfect velocity tracking is assumed and it is not true practically.

Remark 9. About tuning of the fuzzy memberships (cfr. Fig. 2), one considers the initial conditions of the reference and of the actual positions and orientations. So we have initial values of the motion errors (21). Due to the asymptotical stability and boundedness of the errors above (cfr. theorems 1 and 2), one choices a range of the inputs between zero and the initial values above. In this sense the fuzzy memberships are tuned manually.

IV. ADAPTIVE DYNAMIC MOTION CONTROL EXTENSION

In this section a low level adaptive controller based on *backstepping* method [6], [7] is added to previous fuzzy adaptive high level control for nonholonomic autonomous vehicles. The computed torque controller proposed in [6] requires exact knowledge of the dynamics of the vehicle in order to work properly. Since the dynamical parameters of the model (18) cannot be accurately known, an adaptive mechanism is inserted.

Preliminarily important properties of the dynamical model (18) and kinematical model (16) must be presented.

Property 1.b. The *linearity in the parameters* **p** of the dynamical model (18) is shown:

$$\overline{\mathbf{M}}\dot{\boldsymbol{\eta}} + \overline{\mathbf{V}}_\mathbf{m}(\boldsymbol{\eta})\boldsymbol{\eta} = \mathbf{Y}(\boldsymbol{\eta}, \dot{\boldsymbol{\eta}})\mathbf{p} \quad (49)$$

where the vector $\mathbf{p} \in \Re^l$ and $\mathbf{Y}(\boldsymbol{\eta}, \dot{\boldsymbol{\eta}}) \in \Re^{(n-m)\times l}$ are:

$$\mathbf{p} = [\ p_1\ p_2\ p_3\ ]^T = \begin{bmatrix} b^2c^2m + c^2I + I_w \\ b^2c^2m - c^2I \\ 2bc^3dm_c \end{bmatrix} \quad (50)$$

$$\mathbf{Y}(\boldsymbol{\eta}, \dot{\boldsymbol{\eta}}) = \begin{bmatrix} \ddot{\theta}_r & \ddot{\theta}_l & (\dot{\theta}_r - \dot{\theta}_l)\dot{\theta}_l \\ \ddot{\theta}_l & \ddot{\theta}_r & -(\dot{\theta}_r - \dot{\theta}_l)\dot{\theta}_r \end{bmatrix} \quad (51)$$

The elements of the vector **p** consist of unknown dynamical parameters.

Property 2.b. The kinematical model (16) appears as it follows:

$$\begin{bmatrix} \dot{x}_0 \\ \dot{y}_0 \\ \dot{\phi} \end{bmatrix} = \begin{bmatrix} \frac{r}{2}\cos(\phi) & \frac{r}{2}\cos(\phi) \\ \frac{r}{2}\sin(\phi) & \frac{r}{2}\sin(\phi) \\ \frac{r}{2b} & -\frac{r}{2b} \end{bmatrix} \begin{bmatrix} \dot{\theta}_r \\ \dot{\theta}_l \end{bmatrix} = \begin{bmatrix} \frac{r}{2}\cos(\phi) \\ \frac{r}{2}\sin(\phi) \\ \frac{r}{2b} \end{bmatrix} \dot{\theta}_r + \begin{bmatrix} \frac{r}{2}\cos(\phi) \\ \frac{r}{2}\sin(\phi) \\ -\frac{r}{2b} \end{bmatrix} \dot{\theta}_l$$
$$= \begin{bmatrix} \cos(\phi) & 0 \\ \sin(\phi) & 0 \\ 0 & 1 \end{bmatrix} \begin{bmatrix} \frac{r}{2} \\ \frac{r}{2b} \end{bmatrix} \dot{\theta}_r + \begin{bmatrix} \cos(\phi) & 0 \\ \sin(\phi) & 0 \\ 0 & -1 \end{bmatrix} \begin{bmatrix} \frac{r}{2} \\ \frac{r}{2b} \end{bmatrix} \dot{\theta}_l =$$
$$= \boldsymbol{\Sigma}_1\boldsymbol{\theta}_1\dot{\theta}_r + \boldsymbol{\Sigma}_2\boldsymbol{\theta}_2\dot{\theta}_l \quad (52)$$

where $\boldsymbol{\theta}_1$ and $\boldsymbol{\theta}_2$ are parametric vectors while $\boldsymbol{\Sigma}_1$ and $\boldsymbol{\Sigma}_2$ are vectors whose elements consist of known functions.

Now, by inserting the new fuzzy inference system of the previous sections, the adaptive backstepping technique [7] is reformulated.

From (41) and (48) the fuzzy kinematical adaptive tracking controller model can be written as it follows:

$$\begin{aligned} \boldsymbol{\eta}_c &= \boldsymbol{\eta}_c(\mathbf{e},\overline{\alpha},\overline{\beta}) = \boldsymbol{\eta}_c(\mathbf{q},\mathbf{q}_r,\overline{\alpha},\overline{\beta}) \\ \dot{\overline{\alpha}} &= f_1(\mathbf{e},\overline{\alpha}) = f_1(\mathbf{q},\mathbf{q}_r,\overline{\alpha}) \\ \dot{\overline{\beta}} &= f_2(\mathbf{e},\overline{\beta}) = f_2(\mathbf{q},\mathbf{q}_r,\overline{\beta}) \end{aligned} \tag{53}$$

Also the Lyapunov's function (43) appears as it follows:

$$V_1 = V_1(\mathbf{e},\overline{\alpha},\overline{\beta}) = V_1(\mathbf{q},\mathbf{q}_r,\overline{\alpha},\overline{\beta}) \tag{54}$$

Assumption 1. The adaptive tracking controller (53) exists for the kinematical model (16). Also there is a positive-definite and radially unbounded function V_1 such that:

$$\dot{V}_1 = \frac{\partial V_1}{\partial \mathbf{q}}\dot{\mathbf{q}} + \frac{\partial V_1}{\partial \mathbf{q}_r}\dot{\mathbf{q}}_r + \frac{\partial V_1}{\partial \overline{\alpha}} f_1 + \frac{\partial V_1}{\partial \overline{\beta}} f_2 \le 0 \tag{55}$$

where all the signals are bounded.

The following theorem can be formulated.

Theorem 3: Let (16) and (18) be the kinematical and dynamical model respectively. There is the fuzzy kinematical adaptive control (53). The properties 1.b and 2.b are verified and the assumption 1 is satisfied. The reference linear and angular velocities are bounded functions and the reference angular velocity converges to zero. The following adaptive dynamical control law is chosen:

$$\begin{aligned} \boldsymbol{\tau} &= \begin{bmatrix} \tau_l \\ \tau_r \end{bmatrix} = \overline{\mathbf{B}}^{-1}\left(-\mathbf{K}_d\tilde{\boldsymbol{\eta}} + \mathbf{Y}\hat{\mathbf{p}} - \left(\frac{\partial V_1}{\partial \mathbf{q}}\hat{\mathbf{S}}\right)^{\mathbf{T}}\right) \\ \dot{\hat{\boldsymbol{\theta}}}_i &= \boldsymbol{\Lambda}_i\left(\frac{\partial V_1}{\partial \mathbf{q}}\boldsymbol{\Sigma}_i\right)\tilde{\eta}_i \quad i=1...2 \quad ;\dot{\hat{\mathbf{p}}} = -\boldsymbol{\Psi}\mathbf{Y}^T\tilde{\boldsymbol{\eta}} \end{aligned} \tag{56}$$

where:

τ_l is the control torque applied to the left wheel;

τ_r is the control torque applied to the right wheel;

$\hat{\boldsymbol{\theta}}_i$ is the estimation of $\boldsymbol{\theta}_i$, *i=1,2* (cf. eq. 52);

$\mathbf{Y}$ and $\mathbf{p}$ are given by (50) and (51);

$\hat{\mathbf{p}}$ is the estimation of the dynamical parameters of $\mathbf{p}$ vector;

$\boldsymbol{\Sigma}_i$ (i=1,2) matrices are given by (52), V_1 is given by (44) and satisfies the assumption 1;

$\hat{\mathbf{S}}$ is the Jacobian matrix (cf eq. 16) and it depends on estimated kinematic parameters $\hat{\boldsymbol{\theta}}_i$ for i=1,2;

$\tilde{\boldsymbol{\eta}}$ is given by:

$$\tilde{\boldsymbol{\eta}} = \boldsymbol{\eta}_c - \boldsymbol{\eta} = [\tilde{\eta}_1 \ \tilde{\eta}_2]^T \tag{57}$$

where $\boldsymbol{\eta}_c$ is given by (48) and $\boldsymbol{\eta}$ is the dynamical velocity vector of model (18);

$\mathbf{K}_d$, $\boldsymbol{\Psi}$ and $\boldsymbol{\Lambda}_i$ are simmetric and positive definite matrices.

Then $\tilde{\boldsymbol{\eta}}$ converges to zero.

Proof track. The following Lyapunov function is chosen:

$$V_2 = V_1 + \frac{1}{2}\tilde{\boldsymbol{\eta}}^{\mathbf{T}}\overline{\mathbf{M}}\tilde{\boldsymbol{\eta}} + \frac{1}{2}\tilde{\mathbf{p}}^{\mathbf{T}}\boldsymbol{\Gamma}^{-1}\tilde{\mathbf{p}} + + \frac{1}{2}\tilde{\boldsymbol{\theta}}_1^{\mathbf{T}}\boldsymbol{\Lambda}_1\tilde{\boldsymbol{\theta}}_2 + \frac{1}{2}\tilde{\boldsymbol{\theta}}_2^{\mathbf{T}}\boldsymbol{\Lambda}_2\tilde{\boldsymbol{\theta}}_2 \tag{58}$$

where:

$$\tilde{\mathbf{p}} = \hat{\mathbf{p}} - \mathbf{p}; \quad \tilde{\boldsymbol{\theta}}_1 = \hat{\boldsymbol{\theta}}_1 - \boldsymbol{\theta}_1; \quad \tilde{\boldsymbol{\theta}}_2 = \hat{\boldsymbol{\theta}}_2 - \boldsymbol{\theta}_2 \tag{59}$$

By considering assumption 1, after some calculations, the time derivative of (58) results [7]:

$$\begin{aligned} \dot{V}_2 &= \frac{\partial V_1}{\partial \mathbf{q}}\mathbf{S}_1\boldsymbol{\eta}_c + \frac{\partial V_1}{\partial \mathbf{q}_r}\dot{\mathbf{q}}_r + \frac{\partial V_1}{\partial \overline{\alpha}} f_1 + \\ &+ \frac{\partial V_1}{\partial \overline{\beta}} f_2 - \tilde{\boldsymbol{\eta}}^{\mathbf{T}}\mathbf{K}_d\tilde{\boldsymbol{\eta}} \end{aligned} \tag{60}$$

From the assumption 1 and (60) the signals included in $\ddot{V}_2$ are bounded, therefore, from Barbalat's lemma, the function (60) is uniformly continuous and it can be written:

$$\lim_{t\to\infty}\dot{V}_2(t) = 0 \tag{61}$$

From (46) and (61), it yields:

$$\lim_{t\to\infty}\tilde{\boldsymbol{\eta}}(t) = 0 \tag{62}$$

Remark 10. If we assume the adaptive kinematical controller of the section III only, the perfect tracking velocity hypothesis is considered *i.e.* the control velocity $\boldsymbol{\eta}_c$ is instantaneously applied to the ground vehicle, but it is not true. By inserting the dynamical control, instead, the (62) is satisfied and the velocity of the nonholonomic vehicle converges to control signal after some time due to dynamical effects. This is shown in the next section.

Remark 11. If (62) is satisfied, then boundedness and convergence of the tracking errors (21) are assured.

V. Simulation Results

We first simulate the adaptive fuzzy controller for nonholonomic vehicles in Matlab Simulink environment to verify the asymptotical stability and robustness performance before the experimental implementation. Also we use simulation results to compare our method whit the control system proposed in [7]. In this section two simulations results are shown: the first does not consider disturbance; the second consider disturbance violating the nonholonomic constraints of the vehicle motion. Besides, two controller have been simulated in Matlab environment:

1) a controller with adaptive dynamical extension assuming knowledge of the parameters (25), *i.e.* adaptive control without fuzzy inference system [7];

2) the new controller of this work where the parameters (25) are the outputs of the new fuzzy system of the section III, with the new adaptive kinematical control of the section III .C (cf. eq. 48) and the adaptive dynamical control extension of the Section IV (cf. eq. 56).

So the performances and robustness of the two motion control system are compared.

The kinematical and dynamical parameters of the electric nonholonomic vehicle are the following:

$$b = 0.75m;\ d = 0.3m;\ r = 0.15m;\ m_c = 30kg$$

$$m_w = 1kg;\ I_c = 15.6;\ I_w = 0.005;\ I_m = 0.0025.$$

The parameters of the kinematic controller (24) are the outputs of the fuzzy system. The parameters of the kinematical (41) and dynamical (56) adaptive controllers are:

$$\gamma = 0.005;\ \delta = 20.75;\ K_d = 5;\ \psi = 5 \qquad (63)$$

About the controller without fuzzy inference system, the parameters (25) are chosen as:

$$k_x = k_y = k_\phi = 5 \quad \forall t$$

About the two DC motors, one must consider the following model:

$$\begin{aligned} \boldsymbol{\tau}_m &= \mathbf{K}\mathbf{i}_\mathbf{a} \\ \mathbf{v}_a &= \mathbf{L}_\mathbf{a}\frac{d\mathbf{i}_\mathbf{a}}{dt} + \mathbf{R}_\mathbf{a}\mathbf{i}_\mathbf{a} \\ \mathbf{v}_\mathbf{a} &= \mathbf{G}_v\mathbf{v}_c \\ \boldsymbol{\tau} &= \overline{\mathbf{K}}\boldsymbol{\tau}_\mathbf{m} \end{aligned} \qquad (64)$$

where it is:

$\mathbf{i}_\mathbf{a} = \begin{bmatrix} i_{a1} \\ i_{a2} \end{bmatrix}$ armature currents;

$\mathbf{v}_\mathbf{a} = \begin{bmatrix} v_{a1} \\ v_{a2} \end{bmatrix}$ armature voltages;

$\mathbf{v}_c = \begin{bmatrix} v_{c1} \\ v_{c2} \end{bmatrix}$ control voltages;

$\boldsymbol{\tau} = \begin{bmatrix} \tau_r \\ \tau_l \end{bmatrix}$ transmitted command torques to right and left wheels;

$\boldsymbol{\tau}_m = \begin{bmatrix} \tau_{m1} \\ \tau_{m2} \end{bmatrix}$ produced torques;

$\mathbf{K} = 3.34 \times \mathbf{I}\ Ncm/A$ constant torque parameter;

$\overline{\mathbf{K}} = 4 \times \mathbf{I}$ proportionality coefficient between produced and transmitted torque;

$\mathbf{R}_a = 10 \times \mathbf{I}\ \Omega$ armature resistance;

$\mathbf{L}_\mathbf{a} = 0.0241 \times \mathbf{I}\ H$ armature inductance;

and the matrix **I** is an identity matrix with two rows and two columns.

A. *Motion control without disturbance*

n this test the problem of motion control for nonholonomic vehicles is simulated using a feasible, nonholonomic reference trajectory (see Fig. 8).

The initial conditions for the reference position are:

$$(x(0), y(0), \phi(0)) = (0,0,3.48rad) \qquad (65)$$

The initial conditions for the actual vehicle position are:

$$(x(0), y(0), \phi(0)) = (-30,20,5.68rad)\,. \ (66)$$

So the control laws (48) and (56) are simulated suitably.

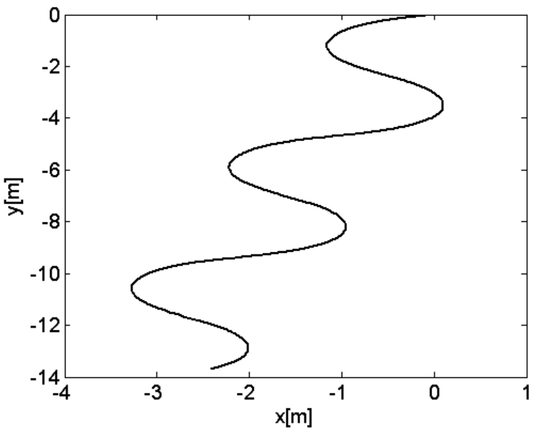

Fig. 8. Reference trajectory x[m], y[m]

Figs. 9, 10 show the tracking errors (21) along x and y directions where we compare the performances of our control system (i.e. fuzzy adaptive motion control) with the performances of the control system proposed in [7] (i.e. adaptive motion control without Fuzzy).

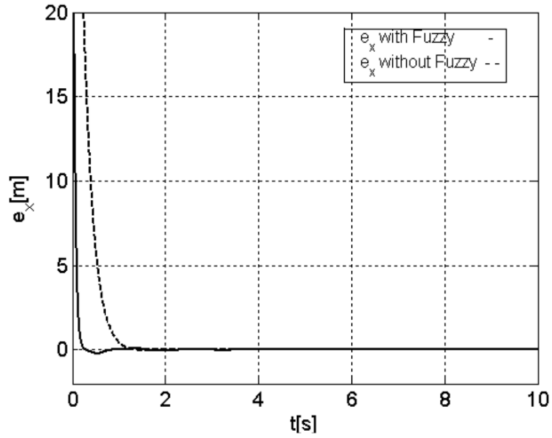

Fig. 9. Longitudinal position error e_x [m] with (-)and without (--) Fuzzy system

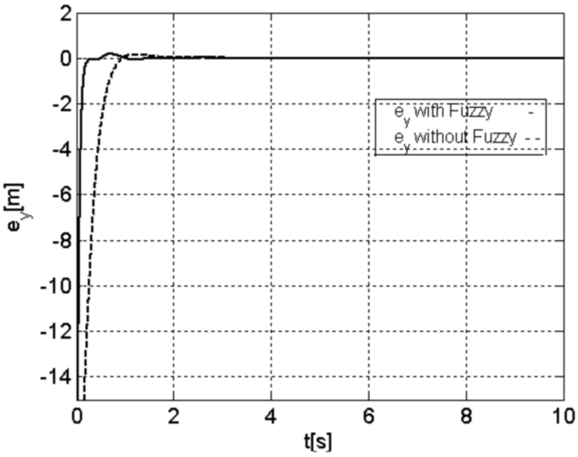

Fig.10. Lateral position error e_y [m] with (-) and without(--) Fuzzy system

The tracking errors resulting from the new fuzzy adaptive control of this work are bounded and converge to zero more rapidly than the tracking errors of the solution one without fuzzy mechanism [7].

Fig. 11 shows the orientation error of the fuzzy adaptive kinematic and dynamic control system, while Figs. 12 and 13 present the estimated kinematical parameters $\overline{\alpha}$, $\overline{\beta}$ (cf. eq. 41) and the dynamical parameters of $\hat{\mathbf{p}}$ vector (cf. eqs. 51 and 56) respectively.

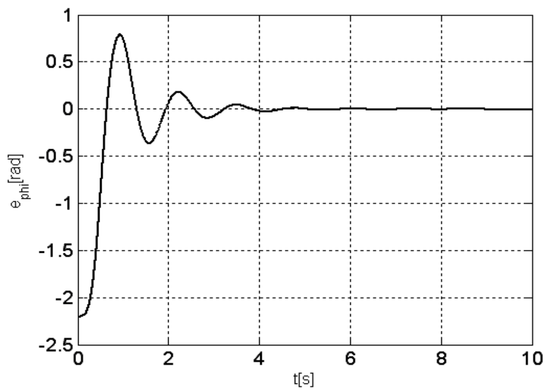

Fig. 11. Orientation error with Fuzzy system, e_{phi} [rad]

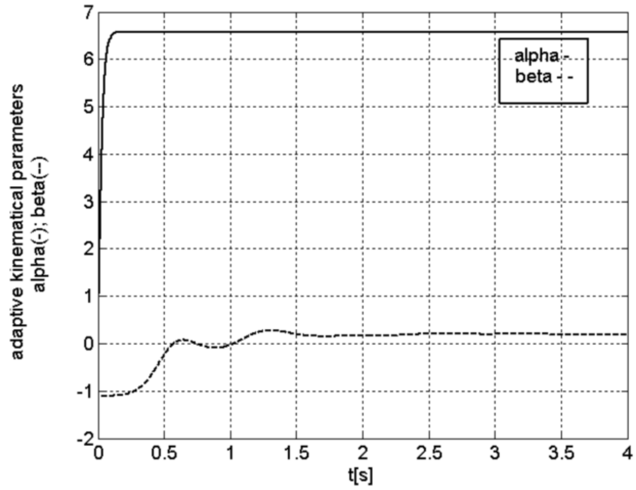

Fig. 12. Adaptive kinematic parameters

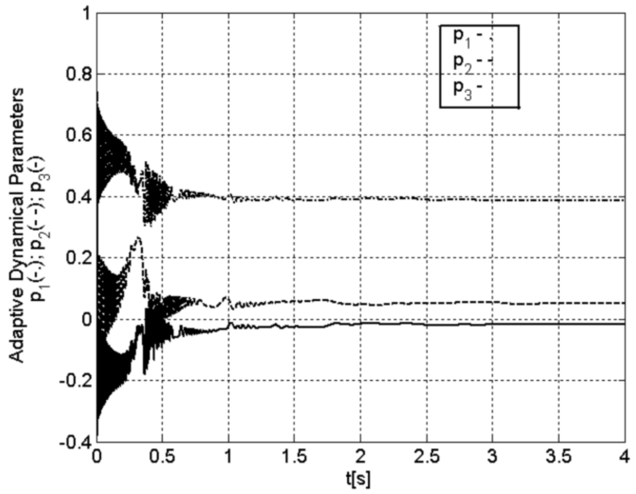

Fig. 13. Adaptive dynamical parameters

Remark 12: From fig. 11 it is evident that the trajectory of the robot reach the trajectory with inclination which leads to an overshoot of near 45 degrees on then a posterior correction goes t near -25 degrees. In fact note that the mass of the ground vehiche is 30Kg, so that the vehicle is not a bigger one. In any case the control strategy may be applied for a variety of vehicles, by varying the input-output values of the memberships fuzzy. The experiment of this paper have been developed for small vehicles.

From Fig. 11 it is evident that the orientation error is bounded and converges to 0 rad.

From Figs. 12 and 13 we observe that the adaptive control is direct, because the estimated parameters are not physical values, but the steady state parameters are constant and the tracking errors of Figs. 9, 10 and 11 converge to zero.

Remark 13. Note that all the absolute tracking errors values of the simulation tests (see Figs. 9, 10, 11) are in the range of the numerical inputs of the fuzzy system (see Fig. 2). In fact the fuzzy map was adjusted based on the control performance as it is explained in remark 9.

Fig. 14 shows the velocity error (57) between the dynamic velocity of the vehicle and the fuzzy control velocity (48). As discussed in remarks 8 and 10, due to dynamical effects, the physical velocity of the vehicle tracks the fuzzy control velocity only after some times. The motion control reacts in a good way and, after some time instants, the velocity error (57) converges to zero. In other words the kinematic control signals cannot affect the vehicle velocities instantaneously.

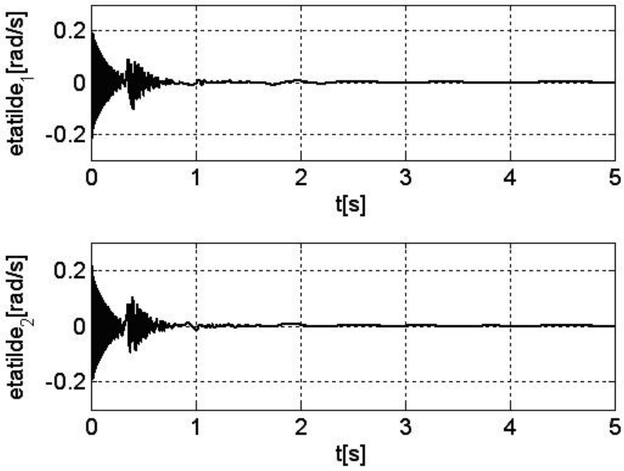

Fig. 14. Tracking velocity error $\tilde{\boldsymbol{\eta}}$ [rad/s]

Now the electrical vehicle has motors installed in two wheels. The model of the motor has been shown in (64). From our simulations, the control torques (cf. eq. (56)) for the left and right wheels can be known precisely and therefore we can estimate the currents for the motors. Based on the experimental system explained in the next section, we consider an amplification between the transmitted and the produced torques equal to 4. So fig. 15 shows the estimated armature currents for right and left motors.

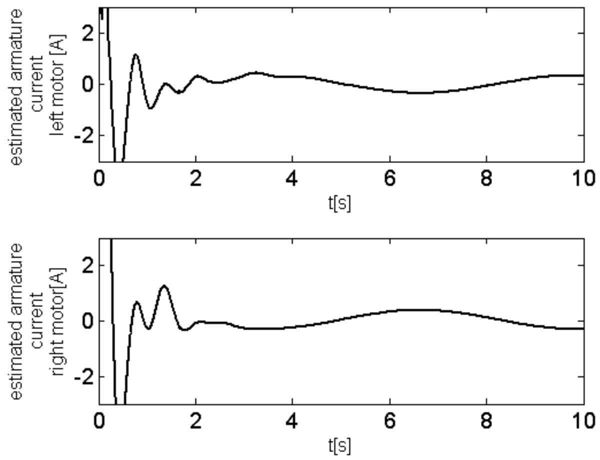

Fig. 15. Estimated armature currents of left and right motor

B. Motion control with disturbance violating non-holonomic constraints

This simulation test shows the robustness of the Fuzzy adaptive motion control system with respect outside disturbances violating the nonholonomic constraints (9). The disturbance above can be caused by the impact of the vehicle with the external environment, as for example the road conditions and the contact between the wheels and the ground where the vehicle moves. In this sense the dynamic model (18) has a bounded unknown disturbance term $\boldsymbol{\tau}_d$ including unstructured dynamics. Now effects of the disturbances above, i.e. perturbations of the actual trajectory of the vehicle, are considered only. So the simulation test consists of generating the slipping of the wheels by a step disturbance of the actual lateral position *y* of the vehicle for every 5s. The reference trajectory is shown in Fig. 8 and it is feasible, i.e. it does not violate the nonholonomic constraints. Fig. 16 shows the tracking error along *y* direction in case of control with and without Fuzzy system. In case of control without Fuzzy system, the parameters (25) are fixed as it results in (63). As discussed in remark 2 it is evident that, with respect to the itself control without Fuzzy inference [7], the adaptive Fuzzy control system of our paper reacts to the disturbance, recovering the vehicle motion with a very good control effort.

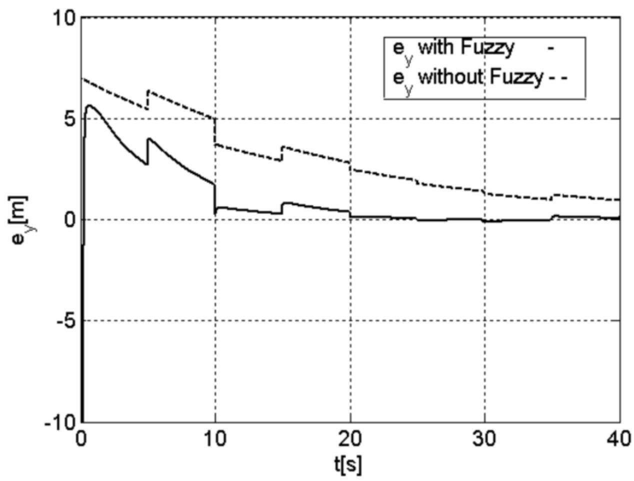

Fig. 16. Lateral position error e_y [m] with (-) and without (--) Fuzzy system

VI Experimental Results

In this section a motion control experiment has been established based on the fuzzy control laws (48) and (56). Experimentation is performed on a vehicle with the same dynamical and kinematical parameters of the simulations.

A. Main technical aspects of the nonholonomic vehicle and of the implemented fuzzy adaptive control system

The details of our vehicle are shown in Fig. 17. The vehicle above is constituted by a mechanical support of circular form, under which two independent traction axis have been installed (differential drive actuation). The informations on linear and angular velocities and therefore on position and orientation of the vehicle have been obtained by two proprioceptive sensors, i.e. one encoder for each wheel.

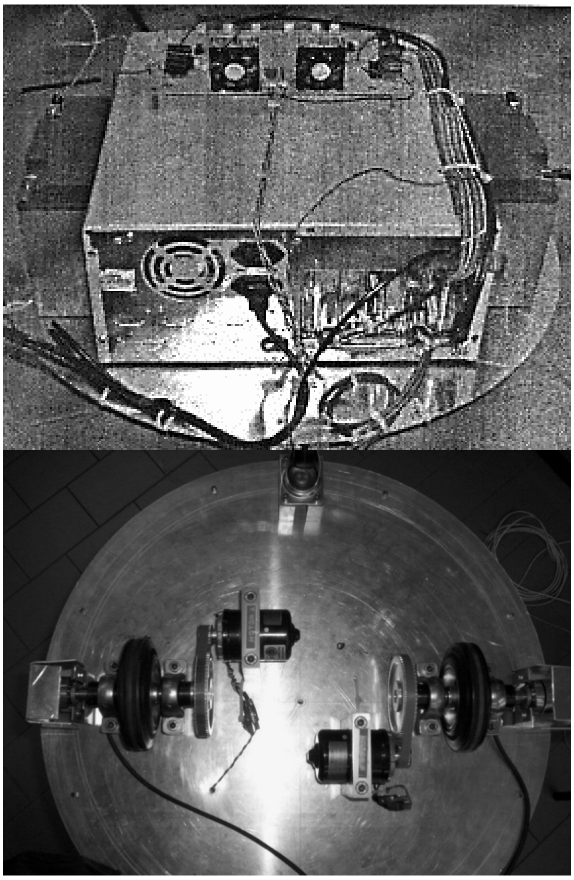

Fig. 17. Nonholonomic vehicle top and rear views: PC target and independent traction axis.

The electric motors are controlled by on board personal computer (PC Target) with Pentium Processor. The signals for the actuators are PWM type. Therefore drivers for the motors have been installed. The motors and the drivers require a set of two on board batteries of 12 V.

Principal components of the experimental system are:

two DC motors;

two encoders Baumer, BHK series;

two drivers LMD18200;

PC Target on board with Encoder Card PCL-833, Multifunctional Card PCL-1800

We use another PC (host computer) for motion control, where the adaptive fuzzy motion controller has been implemented by using Matlab Simulink.

About the motors, they have been chosen for the good torques and robustness performance. The parameters of the model have been shown in the simulation section. The main characteristics of the motors are:

Nominal tension value: 24 V

Nominal current value: 2.8A

Continuous torque: 6 Ncm

Constant torque-current: 3.34 Ncm/A

The employed drivers produce current for the motors to generate the torques. However the drivers above assure maximum current of 3A for the motors with consequential very low torque. So we do not change the driver, but we use a system of motor-axis pulley (see Fig. 18) introducing an amplification between the produced and the transmitted torque. To use the driver LMD18200, the amplification above is 1:4.

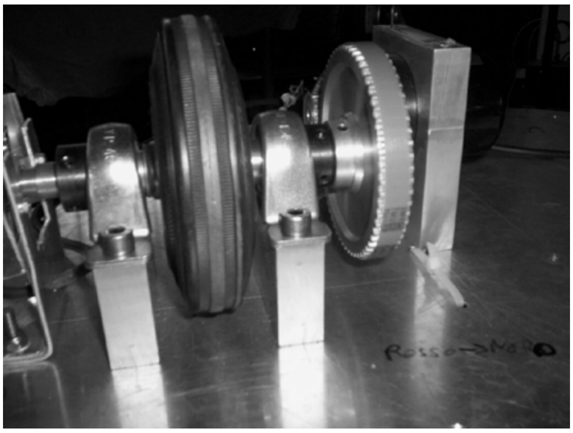

Fig. 18. Motor axis pulley local view

The circuit for the PWM generation has been shown in Fig. 19. In our experimental system the card above is positioned upon the PC target (see Fig. 17-top view). Note that the LMD18200 has three input: PWM, DIR and BRAKE. The brake input can be controlled by microcontroller. In our experiments the input above is not used. So it is “ground”. The input “DIR” is the direction of the motor rotation. Now the multifunctional card PCL-1800 has A/D converter, buffer FIFO of 1Kword, two converters D/A 12 bit, 16 digital inputs and 16 digital outputs. From the D/A of the PCL-1800, reference voltages proportional to the currents are obtained. The card above has been employed to monitor the armature currents, the reference voltages and the current signs. So the difference between the current reference and the measure current feedback is fed into a current control block. Hence, it generates the duty ratio for the PWM converter which provides bidirectional current control of the DC motors.

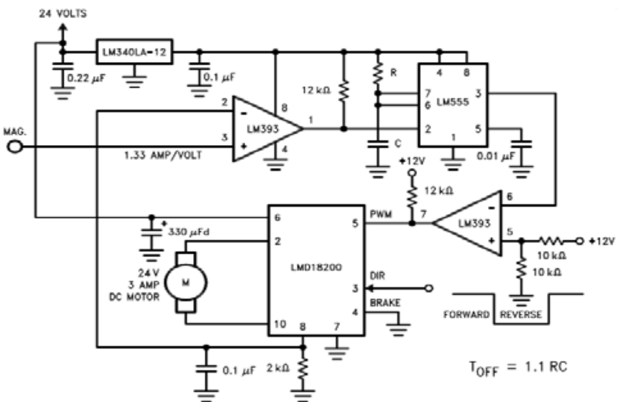

Fig. 19. PWM generation for driver LMD18200

The encoders have been employed to evaluate the velocity rotation of the axis. They use two pulse trains, 90 degree out of phase.

The host computer loads to the PC Target of the vehicle the program and the reference trajectory, while the PC Target communicates to it some variables, as for example the actual position. The host PC reads motor positions for use in graphics routines by using matlab software. The PC target passes latest position to the fuzzy control algorithm implemented in the host PC using matlab simulink. So the Fuzzy control algorithm calculates the new outputs for the DAC of the PCL-1800 generating the reference voltage and waits for the next command from the PC target.

About the software implementation of the fuzzy control laws (48) and (56), the system has been realized by using Matlab Simulink, RealTimeWorkShop and XpcTarget toolboxes. In particular we have used Matlab Simulink to implement the dynamical and kinematical fuzzy controllers and the blocks for the card I/O interfaces. So, by employing RealTimeWorkShop toolbox, the blocks above are converted in C language suitably. The executable code is generated by using *Visual C* Compilator. Therefore the code above is downloaded in the PC target, where there is a real-time operative system. So we monitor the parameters in the remote PC by graphical routines of Matlab.

Fig. 20 shows the block diagram for the acquisition of the encoders data, i.e. angular velocities of the right and left wheels. The data above are downloaded in the host PC. So, by using matlab simulink blocks to implement equation (16), they are processed to obtain the feedback signal and the motion errors (21) of the control system.

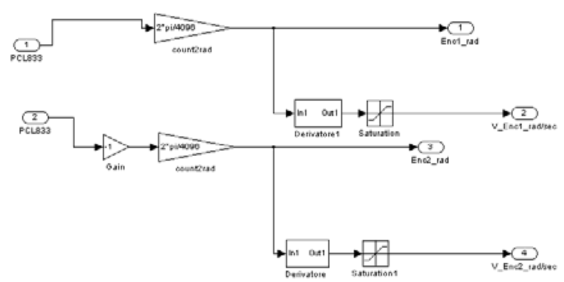

Fig. 20. Interface for data acquisition from encoders

In conclusion the control architecture has three levels:

- from the positions errors (21), the adaptive fuzzy kinematic control generates the speed control (cf. eq. 48);

- from the velocity error (57), the adaptive dynamic control generates the desired torque commands (cf. eq. 56);

- actuation of the torques above by the PCL-1800 with generation of error between the reference and the measured current

for the PWM input generation of the driver LMD18200.

B. Results

In this section experimental results are shown to confirm the simulation results. In the host computer we have implemented a reference curvilinear trajectory. The trajectory above is shown in Fig. 21 and it is equal to the curvilinear length of the simulation tests (see Fig.8). The initial conditions of the reference trajectory and of the vehicle position are the same of the simulation tests (cf. eqs. 65, 66).

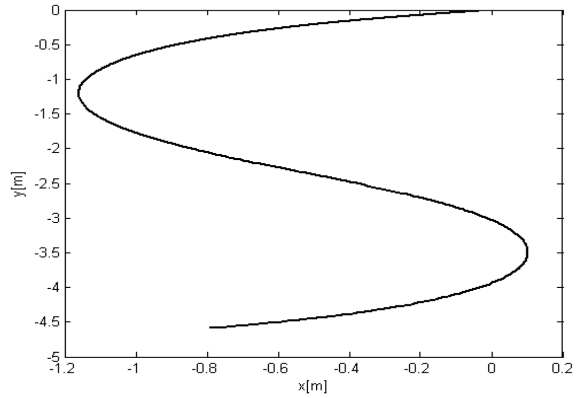

Fig. 21. Reference trajectory

By using the fuzzy control laws (48) and (56), time after time, we have monitored the actual position of the vehicle. Figs. 22 and 23 show the experimental results of the system output response to the reference trajectory of Fig. 21. In particular the reference and experimental actual trajectories along x direction versus time are shown in Fig. 22, while Fig 23 shows the same functions along y direction versus time. To compare experimental and simulation results directly, it is evident that the vertical distances between the trace of the actual and of the reference trajectories (see Figs. 22, 23) represent the longitudinal and the lateral tracking errors. The values of the distances above are similar to the values of the simulation results (see Figs. 9 and 10).

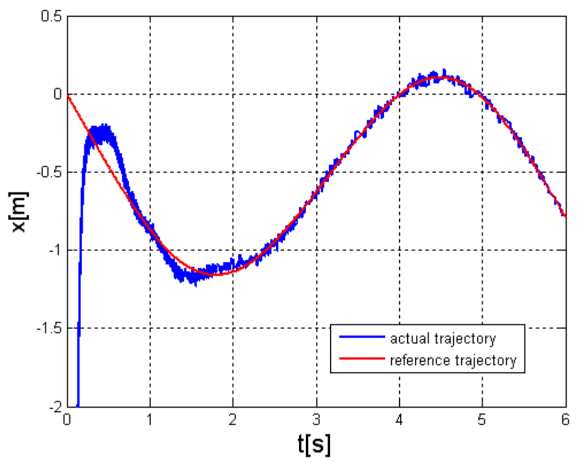

Fig. 22. Reference and actual experimental trajectory along x direction

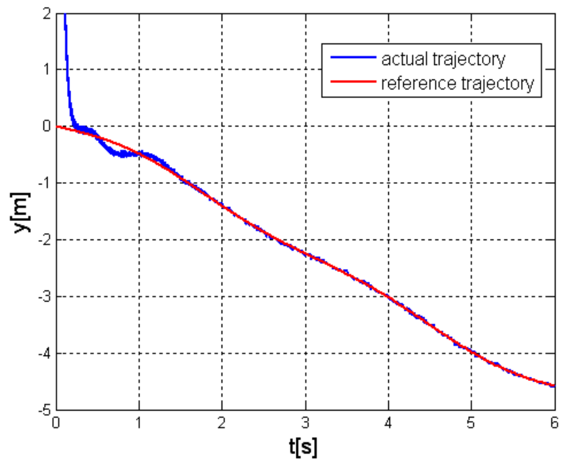

Fig. 23. Reference and actual experimental trajectory along y direction

Figs 24 and 25 show the reference voltages and the sign of the currents for the left and right motors respectively. The informations above come from output DAC of PCL 1800 card.

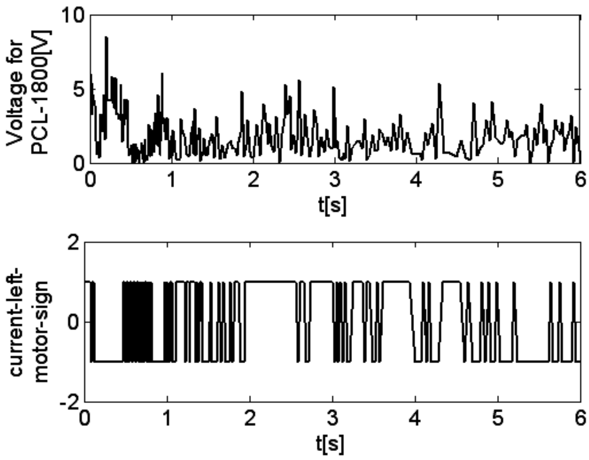

Fig 24. Reference voltage and current left-motor sign from PCL 1800 card.

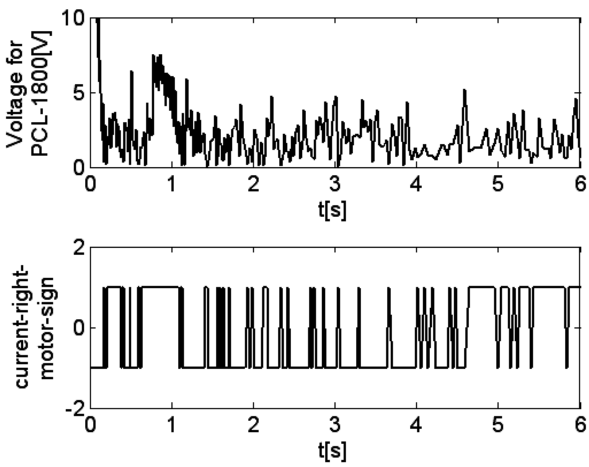

Fig 25. Reference voltage and current right-motor sign from PCL-1800 card.

Fig. 26 shows the measured armature currents for right and left motors. Note that the driver may done 3A max to the motors. The measured armature currents of Fig. 26 are similar to the simulation results of Fig. 15.

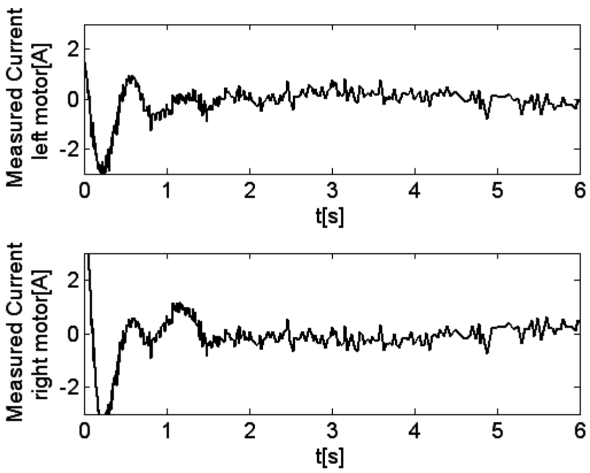

Fig. 26. Measured armature currents

CONCLUSIONS

In this paper an evolution of the adaptive control for motion control of autonomous nonholonomic vehicles by inserting a new Fuzzy inference system has been presented. In particular the fuzzy inference determines the parameters of the kinematic controller with better performance than the adaptive controller without fuzzy proposed in [7]. An adaptive mechanism on line estimated the unknown dynamical and kinematical parameters of the vehicle model. Also, by using the dynamical extension, it is evident that the hypothesis of perfect velocity tracking cannot be satisfied because it is not true practically. Our concepts are formulated to have the asymptotical stability of the tracking errors through Lyapunov's theory and Barbalat's Lemma. The stability results are based on the input-output properties of the fuzzy inference system. Based on theoretical and simulation results we conclude:

- Lyapunov's stability theory can be effectively applied to determine the properties of Fuzzy system for problem of motion control of nonholonomic vehicles;
- the Fuzzy adaptive approach of this paper reduces the response time of the tracking errors with respect to controller without Fuzzy inference mechanism [7];
- the simulation results show the robustness, the asymptotical stability and the fast convergence of the motion errors;
- the experimental results confirm the validity of the proposed method.

REFERENCES

[1] Aicardi M., Casalino G., Bicchi A., Balestrino A., "Closed Loop Steering of Unicycle-Like Vehicles

via Lyapunov Techniques", *IEEE Robot. Automatic. Mag*., vol. 2, 1995, pp. 27-35.

[2] Bentalba S., Hajjajj A, Rachid A., "Fuzzy Control of a Mobile Robot: a New approach", *Proceedings of the IEEE Conference on Control Applications*, 1997, pp. 69-72.

[3] Calcev G., "Some Remark on the Stability of Mamdani Fuzzy Control System", *IEEE Transaction on Fuzzy Systems,* Vol. 6, No. 3, 1998, pp. 436-442.

[4] Corradini M.L., Leo T., Orlando G., "Robust stabilization of a mobile vehicle violating the nonholonomic constraint via quasi-sliding modes", *Proceedings of the American Control Conference,* 1999.

[5] De Sousa C., Hemerly E.M., "Adaptive Control for Mobile Robot using Wavelet Networks", *IEEE transaction on System, Man, and Cybernetics,* vol 32, 2002, pp. 493-504.

[6] Fierro, Lewis, "Control of a Nonholonomic Mobile Robots: Backstepping Kinematics into Dynamics", *J. Robot. Syst.,* vol. 14, no.3, 1997, pp. 149-163.

[7] Fukao T., Nakagawa H., Adachi N., "Adaptive Tracking Control of a Nonholonomic Mobile Robot", *IEEE Transactions on Robotics and Automation,* Vol. 16, Issue 5, 2000, pp. 609-615.

[8] Gang T., "A Simple Alternative to the Barbalat Lemma", *IEEE Transaction on Automatic Control*, Vol. 42, No 5, 1997.

[9] Grartner H., Astolfi A., "Stability study of a fuzzy controlled mobile robot", *Proceedings of the 35th IEEE Conference on Decision and Control,* 1996.

[10] Indiveri G., "An Introduction to Wheeled Mobile Robot Kinematics and Dynamics*", University of Lecce-DII, Department of Innovation Engineering,Robocamp-Paderborn* (Germany), 2002.

[11] Lam K.H., Lee H.T., Leung F.H.F, Tam P.K.S., "Fuzzy model reference control of wheeled mobile robots", *Proceedings of 27th IEEE Conference on Industrial Electronics society, IECON*, 2001, pp. 570-573.

[12] Lee H.T., Lam H.K., Leung F.H.F., Tam P.K.S., "A Practical Fuzzy Logic Controller for the Path Tracking of Wheeled Mobile Robots", *Proceedings of 27th IEEE Conference on Industrial Electronics IECON* , 2001, pp. 574-579.

[13] Leo T., Orlando G., "Robust Discrete Time Control of a Nonholonomic Mobile Robot", *Proceedings of 14th IFAC World Congress,* 1999, pp. 137-142.

[14] Llama M.A., Kelly R., V. Santibanez, "Stable Computed-Torque of Robot Manipulator via Fuzzy Self Tuning", *IEEE Transactions on Systems, Man, and Cybernetics,* Vol. 30, No.1, 2000, pp. 143-150.

[15] Raimondi F.M., Melluso M., "A Neuro Fuzzy Controller for Planar Robot Manipulators", *WSEAS Transactions on Systems,* Issue 10, Vol.3, 2004, pp. 2991-2997, Inspec IEE.

[16] Raimondi F.M., Melluso M., Ciancimino L.S, "A new kinematic and dynamic direct adaptive fuzzy control of constrained mobile wheeled vehicles", *Proceedings of IEEE Conference on ETFA 2005*, vol. 2., , 2005, pp. 181-188.

[17] Schuster G., "Simulation of Fuzzy Motion Controlled four wheel steered mobile robot", *Institute of Instrumentation and Automation,* Budapest, 2000.

[18] Sugeno M., Taniguchi T., "An Improvement of Stability Conditions for Continuous Mamdani-Like Fuzzy Systems", *IEEE Transactions on System, Man, and Cybernetics,* vol. 34 No. 1, 2004.

[19] Yamamoto Y., Yun X., "Coordinating Locomotion and Manipulation of a Mobile Manipulator", *Proceedings of 31th IEEE Conference on Decision and Control,* 1992*,* pp. 2643-2648.

[20] Wilson D.G., Robinett R.D., "Robust Adaptive Backstepping Control for a Nonholonomic Mobile Robot", *Proceedings of IEEE International Conference on Systems, Man and Cybernetics,* vol.5, 2001, pp. 3241-3245.

[21] Zhu C., Rajamani R., "Global Positioning System-based Vehicle Control for Automated Parking", *Part D: Journal of Automobile Engineering*, vol. 220, 2006, pp. 37-52.